

Light-induced defect states in hydrogenated amorphous silicon centered around 1.0 and 1.2 eV from the conduction band edge

J. M. Pearce, J. Deng, R. W. Collins, and C. R. Wronski

Center for Thin Film Devices, The Pennsylvania State University, University Park, Pennsylvania 16801

(Received 10 July 2003; accepted 12 September 2003)

To take into account the presence of multiple light-induced defect states in hydrogenated amorphous silicon (*a*-Si:H) the evolution of the entire spectra of photoconductive subgap absorption, $\alpha(h\nu)$, has been analyzed. Using this approach two distinctly different light-induced defect states centered around 1.0 and 1.2 eV from the conduction band edge are clearly identified. Results are presented on their evolution and respective effects on carrier recombination that clearly point to the importance of these states in evaluating the stability of different *a*-Si:H solar cell materials, as well as elucidating the origin of the Staebler–Wronski effect. © 2003 American Institute of Physics. [DOI: 10.1063/1.1624637]

Light-induced (LI) degradation in hydrogenated amorphous silicon (*a*-Si:H) is not only of scientific but also of technological interest because of its limitations on the performance of *a*-Si:H-based solar cells. Materials for solar cells have been extensively studied and the results on the LI gap states measured on thin films are used to predict the stability and performance of the solar cells. Because LI degradation is generally associated with the creation of dangling bonds, the emphasis has been on determining their evolution under illumination.¹ Although the neutral dangling bond (D^0) defect density can be directly measured with electron spin resonance (ESR) the most commonly used method is photoconductive subgap absorption as a function of photon energy $\alpha(h\nu)$. Generally, $\alpha(h\nu)$ is interpreted solely in terms of D^0 defect states, where their densities are directly related to the magnitude $|\alpha(h\nu)|$, typically for $h\nu$ 1.1 to 1.3 eV. Such an approach has been used to explain a plethora of results on LI changes in carrier recombination and their annealing. However, results have also been reported that point to the introduction of other defect states and that $\alpha(h\nu)$ cannot be interpreted in such a simple manner.² This includes the widespread range of relationships found between light-induced changes in $|\alpha(h\nu)|$, N_D^0 as measured by ESR, and electron mobility lifetime ($\mu\tau$), as well as the absence of any correlations with the fill factors (FFs) of solar cells.^{3–5} In this letter, contributions to the $\alpha(h\nu)$ of multiple defect states at and below midgap are addressed by analyzing the evolution of the entire spectra rather than just their magnitude. Although any direct correlation of these defect states below midgap with the carrier recombination is limited by the presence of states above midgap, two distinctly different light induced defect states centered around 1.0 and 1.2 eV from the conduction band (CB) edge are clearly identified and their evolution found to be consistent with the corresponding changes in $\mu\tau$.

The results presented here are on two materials having radically different microstructure and consequently degradation kinetics. One is a protocrystalline material deposited with $R=[H_2]/[SiH_4]=10$ at a deposition rate of 0.5 Å/s, and the other is an undiluted $R=0$ material deposited at a rate of 20 Å/s.^{6,7} The photoconductive subgap absorption, for $h\nu$ 0.9

to 1.5 eV, was measured using the dual-beam photoconductivity method,⁸ and the absolute values of $\alpha(h\nu)$ obtained with a normalization procedure to transmission and reflection measurements developed by Jiao *et al.*⁹ The studies were carried out on 1- μ m-thin films, and the electron $\mu\tau$ products were measured with volume absorbed light. Both the $\alpha(h\nu)$ and $\mu\tau$ measurements were carried out at 25 °C with the LI changes obtained under 1 sun illumination with tungsten-halogen lamps with IR filters.

Shown in Fig. 1 are the $\mu\tau$ products at carrier generation rates of 10^{19} cm⁻³ s⁻¹ for the two materials in the annealed state (AS) and their changes under 1 sun illumination at 25 °C. Also shown are the $\mu\tau$ products for the $R=10$ material at 75 °C. It can be seen in Fig. 1 that in the AS, the $\mu\tau$ product of the $R=10$ material is about five times higher than in the $R=0$ material, as is generally expected for better quality materials. Although there is a similarity in the kinetics of

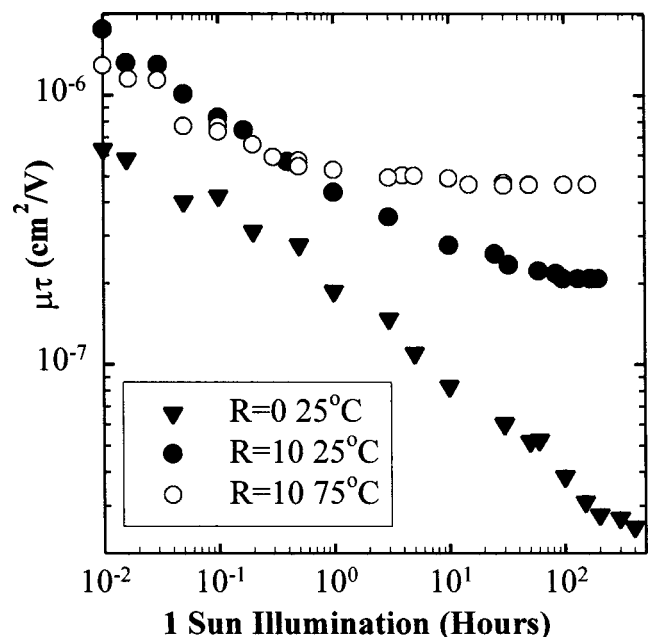


FIG. 1. Electron mobility lifetime products as a function of exposure to 1 sun illumination time for $R=0$ and $R=10$ materials at 25 °C and for the $R=10$ material at 75 °C.

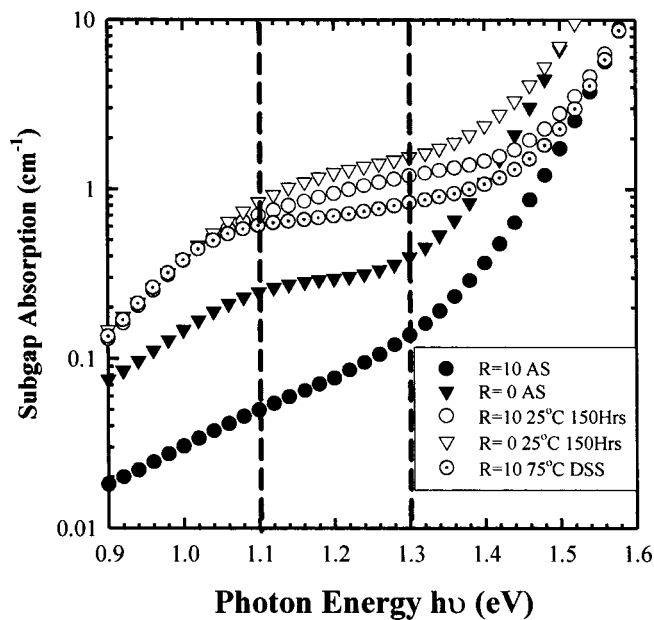


FIG. 2. Subgap absorption as a function of photon energy for the $R=0$ and $R=10$ materials in the AS and after 150 h of 1 sun illumination at 25 °C, and the $R=10$ film in a DSS at 75 °C.

their initial LI changes, there is a marked difference in their evolution towards a degraded steady state (DSS). At 25 °C, the protocrystalline material attains a DSS in approximately 100 h, whereas in the $R=0$ material, the commonly reported kinetics with $\sim t^{-1/3}$ extends for 400 h with no approach to DSS. It should be noted here that after 150 h, the $\mu\tau$ product are \sim ten times higher in the $R=10$ than in the $R=0$ material. When the temperature of degradation is raised to 75 °C, there is virtually no change in the kinetics of the 20 Å/s material, whereas the $R=10$ reaches a DSS with a $\mu\tau$ values that is \sim two times higher than at 25 °C.

In Fig. 2, the $\alpha(h\nu)$ spectra are shown for the two materials in the AS, as well as after 150 h of degradation at 25 °C. Also shown are the results for the DSS of the $R=10$ film degraded at 75 °C. The effects of the valence band states on $\alpha(h\nu)$ spectra can be observed above 1.3 eV, where the values for the two materials differ because of their bandgaps ($E_{\alpha 2000}$), which are 1.86 and \sim 1.80 eV for the $R=10$ and $R=0$ materials, respectively. In the AS, the $|\alpha(h\nu)|$ in the region from 1.1 to 1.3 eV, commonly used in evaluating $\alpha(E)$, is \sim four times lower than that of $R=0$ material. Although this is consistent with the values of $\mu\tau$, it is important to note the striking difference between the shapes of the $\alpha(h\nu)$ spectra. The $R=0$ spectrum has the commonly found shoulder, whereas the $R=10$ continually decreases with $h\nu$ due to its protocrystalline nature. This clearly indicates a significant difference in the intrinsic gap states of the two materials.

In the degraded states, the differences between the various spectra are subtler since they have similar values of $\alpha(h\nu)$. After 150 h of illumination at 25 °C, the $R=0$ film clearly develops a shoulder similar to that in the $R=0$ material. The $|\alpha(h\nu)|$ values in the region 1.1 to 1.3 eV in the two materials are consistent with those of $\mu\tau$, higher $|\alpha(h\nu)|$ values correspond to lower $\mu\tau$ values. However, the small difference of \sim 30% in $\alpha(1.2$ eV) is completely inconsistent with the difference of a factor of 10 in the $\mu\tau$ products.

Similarly, the reduction in $\alpha(1.2$ eV) values of the $R=0$ material in the 75 °C DSS is consistent with the corresponding higher values of $\mu\tau$, but not by the factor of >2 . Since for the $R=0$ material, no difference in $\mu\tau$ kinetics is present between 25 and 75 °C, as expected, there were none in the $\alpha(h\nu)$ spectra. It is quite apparent from the results just discussed that the evolution of multiple defect states has to be taken into account in interpreting $\alpha(h\nu)$ spectra. This becomes even more evident from the $\alpha(h\nu)$ spectra for $h\nu < 1.1$ eV, which, as can be seen in Fig. 2, are virtually identical despite the large differences in the corresponding $\mu\tau$ products.

Any interpretation of $\alpha(h\nu)$ in terms of the density and energy distribution of multiple defect states is complicated by the nature of photoconductive subgap absorption, which is determined by $N(E)$, the densities of electron occupied states, and not directly by the total defect density N_{DEF} . Photoconductive subgap absorption is determined from the absorption of photons, which excite electrons into the extended states in the CB, whose density is then measured as the generated photocurrent. Thus, for any given photon energy, $\alpha(h\nu)$ is a measure of the number of electrons excited into the CB (E_C) which are located within $h\nu$ of E_C and is given by⁹

$$\alpha(h\nu) = k(h\nu)^{-1} \int N(E) N_{\text{CO}}(E + h\nu - E_C)^{1/2} dE. \quad (1)$$

The integral takes into account that $h\nu$ can excite electrons located $E_C - E < h\nu$. $N_{\text{CO}}(E - E_C)^{1/2}$ is the parabolic distribution of extended states in the CB. k depends on the dipole matrix elements for transitions from localized to extended states and is assumed to be constant.¹⁰ In the case of a single type of defect state, it is possible to relate $N(E)$ to $N_{\text{def}}(E)$ directly because the occupation of these states is constrained by charge neutrality. However, in the case of multiple defect states the electron occupation of each type of state is determined by the kinetics of carrier recombination and depends not only on their energy distribution in the gap, but also on their relative densities and capture cross sections of the states.¹¹ Despite these complexities, information can be obtained about the evolution of the light-induced defects (LIDs) and in particular their energy distributions. In order to relate $\alpha(h\nu)$, which includes the contributions from all the electron-occupied states at energies within $h\nu$ from E_C , to the energies of the defect states relative to E_C , it is necessary to take the derivative of the $\alpha(h\nu)$ spectra. In the case when $N(E)$ change rapidly with E , such as a Gaussian distribution, the effect of $N_{\text{CO}}(E - E_C)^{1/2}$ on the joint density of states is small. Consequently, the derivative of Eq. (1) yields

$$kN(E) = (h\nu) d[\alpha(h\nu)]/dE - \alpha(h\nu). \quad (2)$$

The evolution of the LI gap states can be characterized by normalizing the values obtained from Eq. (2) for $kN(E)$ after degradation to that in the AS, yielding

$$P(E) = kN_{\text{DS}}(E)/kN_{\text{AS}}(E) = N_{\text{DS}}(E)/N_{\text{AS}}(E). \quad (3)$$

The $P(E)$ spectra obtained from the results in Fig. 2 are shown in Fig. 3, where their magnitude represents the increase in the densities of electron-occupied states at different energies in the gap from the AS. Because of the complexities

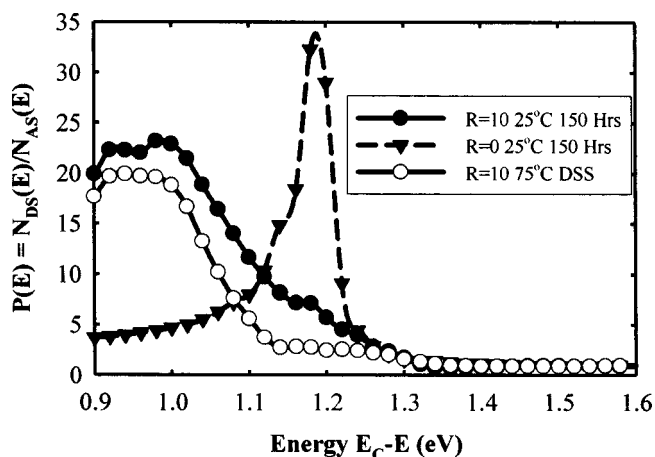


FIG. 3. The $P(E) = N_{DS}(E)/N_{AS}(E)$ spectra as a function of energy from the CB obtained for the results shown in Fig. 2.

mentioned earlier, quantifying the $P(E)$ spectra in terms of $N_{DEF}(E)$ cannot be made without numerical modeling.¹² Nevertheless, it is possible to identify their energy distributions and relate the differences to those in $\mu\tau$, which clearly is not possible for $|\alpha(E)|$. From the results in Fig. 3, the creation of two distinctly different LID states centered around 1.0 and 1.2 eV from E_C can be clearly identified. In the case of the $R=0$ material after 100 h of degradation at 25 °C, there is a predominant contribution from the peak around 1.2 eV that dominates the spectrum, with an almost negligible tail extending towards midgap. In the case of the protocrystalline material, on the other hand, this contribution to the $P(E)$ spectrum is drastically reduced, so that there is now a broad peak centered at 1.0 eV, with only a shoulder at 1.2 eV. The creation of large densities of the LID states in the $R=0$ material around 1.2 eV can be attributed to its poor microstructure due to the fast rate deposition rate. Clearly identifying these states and distinguishing them from those around 1.0 eV cannot be as readily done in materials deposited at slow rates. This enormous difference in $P(1.2 \text{ eV})$ between the two films seen in Fig. 3 clearly indicates the presence of a large difference in their gap state, which is then reflected in the factor of 10 difference in their corresponding $\mu\tau$ products. A more quantitative comparison can be made between the contributions of the two states from $|P(E)|$ spectra on the same material under different degradation conditions. It is seen in Fig. 3, that for the $R=10$ material in the improved DSS at 75 °C, there is only a slight reduction in the defect states around 1.0 eV. The much larger suppression of those around 1.2 eV, on the other hand, can explain the $\mu\tau$ values that are a factor of >2 higher. However, since no corresponding information is currently available about the states located above midgap, no definite conclusions can be drawn about the nature of these two defect states.

The results presented here, which identify distinctly different LID states centered around 1.0 and 1.2 eV from E_C and their respective effects on carrier recombination, are consistent with a variety of results which cannot be explained in terms of a single state located around midgap.² Their evolution is also consistent with the presence of “slow” and “fast” defects,^{13,14} as well as with the degradation kinetics of a -Si:H films and cells.¹⁵ Since recently direct correlations have been established between the LI changes in $\mu\tau$ and the FF of corresponding solar cells,¹⁴ it is important, therefore, to take into account the presence of at least these two defect states in evaluating the stability of a -Si:H solar cell materials. No conclusions are drawn here about the defects associated with these states; however, their distinct differences in their creation kinetics cannot be overlooked in the attempts on establishing the origin of the Staebler–Wronski effect.

The authors would like to thank Dr. Matsuda for supplying thin films, Dr. Jiao for helpful discussions, and X. Niu for technical assistance. This research was supported by the National Renewable Energy Laboratory under subcontract NDJ-2-30630-01.

- ¹H. Fritzsche, *Annu. Rev. Mater. Sci.* **31**, 47 (2001).
- ²C. R. Wronski, J. M. Pearce, R. J. Koval, X. Niu, A. S. Ferlauto, J. Koh, and R. W. Collins, *Mater. Res. Soc. Symp. Proc.* **715**, A13.4 (2002).
- ³P. Stradins, S. Shimizu, M. Kondo, and A. Matsuda, *J. Non-Cryst. Solids* **299–302**, 460 (2002).
- ⁴B. von Roedern, *Appl. Phys. Lett.* **62**, 1368 (1993).
- ⁵J. M. Pearce, R. J. Koval, R. W. Collins, C. R. Wronski, M. M. Al-Jassim, and K. M. Jones, *29th IEEE Photovoltaic Specialists Conference Proceedings* (IEEE, New York, 2002), p. 1101.
- ⁶R. Koval, X. Niu, J. Pearce, L. Jiao, G. Ganguly, J. Yang, S. Guha, R. W. Collins, and C. R. Wronski, *Mater. Res. Soc. Symp. Proc.* **609**, A15.5 (2000).
- ⁷M. Kondo, T. Nishimoto, M. Takai, S. Suzuki, Y. Nasuno, and A. Matsuda, *Technical Digest of the 12th International PV Science and Engineering Conference*, Jeju, Korea, 11–15 June 2001, p. 41.
- ⁸L. Jiao, H. Liu, S. Semoushikina, Y. Lee, and C. R. Wronski, *Appl. Phys. Lett.* **69**, 3713 (1996).
- ⁹L. Jiao, I. Chen, R. W. Collins, C. R. Wronski, and N. Hata, *Appl. Phys. Lett.* **72**, 1057 (1998).
- ¹⁰W. B. Jackson, S. M. Kelso, C. C. Tsai, J. W. Allen, and S. J. Oh, *Phys. Rev. B* **31**, 5187 (1985).
- ¹¹A. Rose, *Concepts in Photoconductivities and Allied Problems* (Kreiger, New York, 1978).
- ¹²M. Günes, C. R. Wronski, and T. J. McMahon, *J. Appl. Phys.* **76**, 2260 (1994).
- ¹³L. Yang and L. Chen, *Appl. Phys. Lett.* **63**, 400 (1993).
- ¹⁴J. M. Pearce, R. J. Koval, X. Niu, S. J. May, R. W. Collins, and C. R. Wronski, *17th European PV Solar Energy Conference Proceedings*, Munich, Germany, October 2002, Vol. 3, p. 2842.
- ¹⁵J. Pearce, X. Niu, R. Koval, G. Ganguly, D. Carlson, R. W. Collins, and C. R. Wronski, *Mater. Res. Soc. Symp. Proc.* **664**, A12.3 (2001).